EVALUATING THE UNCERTAINTY OF SPATIAL RAINFALL WITH DUAL-POLARIZED WEATHER RADAR AND GAUGES OBSERVATION

PROJECT - ENVIRONMENTAL SPATIAL DATA ANALYSIS CEE 690-02

STUDENTS: ZILIN YIN, SIKAI ZHENG, CHANGPENG FAN AND LUIZ BACELAR[1]

December 16th, 2019

CONTENTS

[1] *Department of Civil and Environmental Engineering, Duke University, Durham, United States*

LIST OF FIGURES

LIST OF TABLES

1 INTRODUCTION AND STATEMENT OF THE PROBLEM

An accurate precipitation data is highly important to hydrological and weather models applications [12, 6, 4]. The Quantitative Precipitation Estimates (QPE) are high resolution rainfall fields which are able to represent, in a small spatial and temporal scales, their own variability. Usually QPE are based in remote sensing data such as provided by ground weather radars or satellites. Depending on the instruments, there are inerrant errors associated to the precipitation retrieval [1, 3]. For instance, the empirical relationship used by weather radar relies on the measurement of hydrometeros back-scatter to estimates the rainfall fields. The weather radar electromagnetic pulse can be directly affected by the terrain topography, ground clutter or by the presence of non-meteorological targets which makes the information inaccurate and unassertive.

To solve some of the difficulties to estimate the precipitation by reflectivity fields, the QPE is often combined with rain gauge measurements. An automatic rain gauge can provide in real-time the best quantitative rainfall measurement so far, but it fails to represent the spatial variability of the precipitation. Some algorithms take advantage of rain gauges in order to correct the intensity values of a rainfall field derived by weather radars [5, 9**?**]. Even these techniques carry some uncertainties, and different statistical correction methods are applied depending on the structure of the errors.

The spatial and temporal variability of the errors are not always homogeneous, so stochastic methods are currently the best approach to expose the uncertainties in combining weather radar and rain gauges data. Different from an only deterministic corrected field, the stochastic methods offer a probabilistic estimation of the errors. An usual probabilistic analysis applied to this issue is a interpolation of error by geoestatistical methods [12, 4]. The radar-gauge merging can be performed by a kriging of error in a conditional simulation. In this case, the radar rainfall fields use the rain gauge values to quantify the radar error covariance structure. Each possible realization is conditionally generated as a possible scenario of the error spatial distribution. The realizations or simulations are represented by members which in a group represent the ensemble of equally probable fields.

This course project aims to apply a geoestatistical method based on radar-gauge errors as a conditional simulation to QPE fields. The location for this study was chosen based mainly on the necessity of the National Center of Monitoring and Early Warnings of Natural Disasters (Cemaden) to correct their radar fields. The current deterministic weather radar QPE is specially used for rainfall thresholds of landslides in Recife City-PE. It is expected to demonstrate an alternative probabilistic approach to reproduce more accurately 30 minutes, 1 hour and 24 hours accumulated rainfall fields.

1.1 Project Questions and Objectives

The projected aims to evaluate the uncertainties between the rainfall estimated by the weather radar and the rain gauge values. What are the correlations between the data sets in 30 minutes, 1 hour and 1 day accumulated rainfall?

The major objective is to exposure the uncertainties and analyse if, after the conditional simulations, we are able to reproduce the weather radar fields closer the to rain gauge values. Are the conditional simulations enough to capture the spacial variability of the errors ? If not, in which cases?

2 DATA SET: AUTOMATIC RAIN GAUGES NETWORK

An automatic rain gauges network and a dual-polarized weather radar will be the main data set used in this project. The data sets are described as follow.

The data will be provided by the National Center of Monitoring and Early Warnings of Natural Disasters (Cemaden) [1]. The rain gauges network make quantitative measurements of rainfall at every 10 minutes intervals. It is estimated to use more than 100 rain gauges over the weather radar radius, for each rainfall event studied. In a total, it was used 237 rain gauges over the radius of the weather radar.

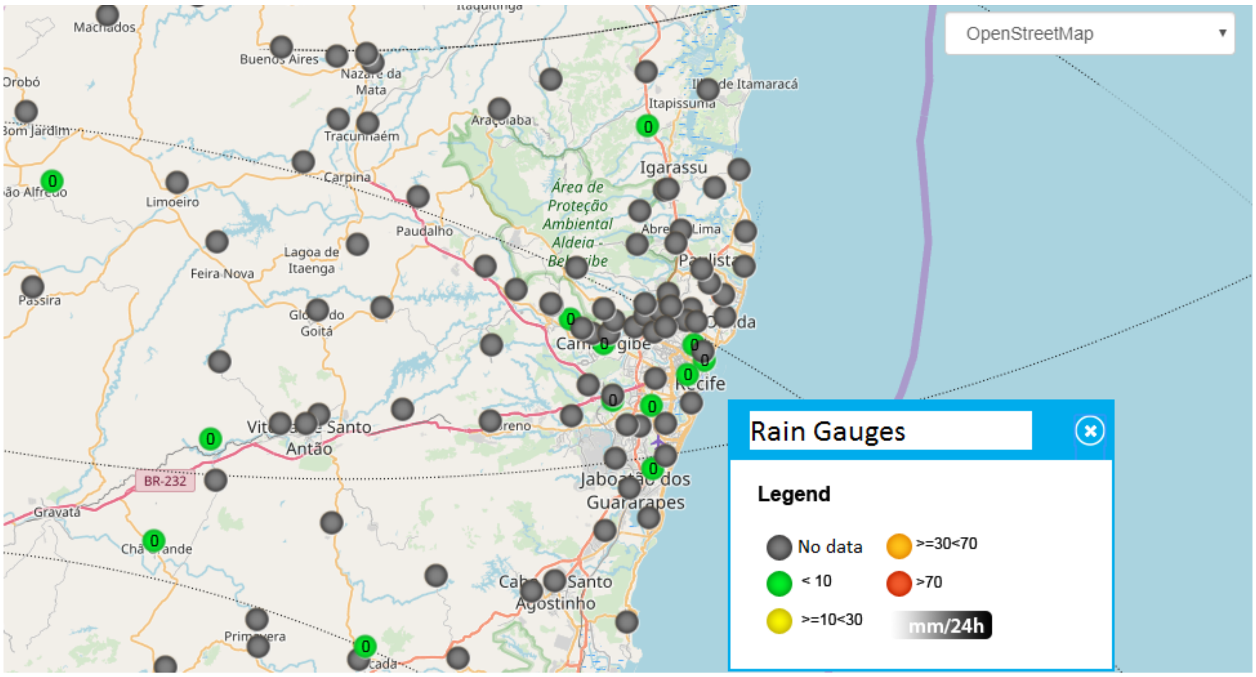

Figure 1: Rain Gauges over the study area. Source: Cemaden

3 DATA SET: DUAL-POLARIZED WEATHER RADAR

3.1 Principal of the measurements

A weather radar is a type of radar used to locate clouds, calculate its motion and classify hydrometeors inside them, for instance, rain, snow or hail. Weather radars send directional pulses of microwave radiation that interact with different targets in the atmosphere. In a dual-polarized system, the pulse is sent and received in both horizontal and vertical orientation. It allows better measurement of the size of the target, which consequently permits better hydrometeors classification.

The weather radar measures the power received P_r (Equation 1) considering a pulse volume in the beam width.

$$P_r = \frac{P_t g^2 \lambda \theta_0^2 c \tau}{1024 \ln(2) \pi^2 r^2} \sum_{vol} \sigma_i \tag{1}$$

1 access in:http://www.cemaden.gov.br/mapainterativo/

As, P_t the received power, g the antenna gain, r the range, θ_0 the half-power beam width, τ the pulse duration, P_t the transmitted power, λ the radar wavelength, σ the scattering cross section and c the speed of light.

If we consider that many of these therms remain constant during the weather radar measurements, what we really want to know is the backscatter in the cross-section or the "reflectivity factor" z of our hydrometeorological targets. So the Equation 1 can be resumed as the Equation 2.

$$z = cp_r r^2 \tag{2}$$

It shows an important idea that the measurement volume increases with the range in a r^2 dependency. The backscattered power z is then converted to Rainfall Rate (R) by using a Z-R relation. As showed by [7] the Z-R relations are not unique and highly depends on the drop size distribution (DSD), which can vary from precipitation type characteristics and weather condition. This is basically because of the chaotic state of the atmosphere. When the micro-physicals dynamics of the hydrometers happens so fast, it is very hard to assume a DSD while process like coalescence, breakup, accretion, evaporation and condensation are constantly affecting the DSD.

The reflectivity factor z is defined as the sum over all scaterring particles assumed to be small compared to the weather radar wavelength and are from water per volume ($1\ m^3$)

$$z = \sum volD^6 \tag{3}$$

The factor D^6 is established by the concept to the distribution in a Rayleigh scatter, where D « λ, and the particles are water. So the reflectivity factor z relative to $1\ mm^6/m^{-3}$ (for example in 1 rain drop D = 1mm), can be assumed when we apply this Equation 4 in units of dBz.

$$Z = 10.log_{10}.\frac{z}{1mm^6m^{-3}} \tag{4}$$

For instance a drizzle would have a value of 10 dBz, while bigger rain drop sizes, like a heavy rain in a thunderstorm, would have a value of 70 dBZ. So, many of our problems to make rainfall retrieval is to assume a DSD when we actually don't have enough measurements (I am saying this in the case of single polarized radar). The reflectivity factor as a function of drop size distribution N(D) 5, can be written as:

$$Z = \int_0^\infty N(D)dD \tag{5}$$

Due to the dependency on the rain drop size distribution $N(D)$ no linear relation between rainfall and reflectivity factor is possible. So we need to fit the $N(D)$ to a known statistical distribution. For example, [7] applied different statistical models to describe the drop size distribution as exponential, gamma and normalized gamma distribution, and how them affect the Z-R relations. The results obtained by [7] provided information which the rain-rate controlled and shape-controlled regimes are located respectively above and below the value of R = 20 mm/h.

The dual-polarized system in a weather radar can have some advantages over the traditional Z-R methods, mainly because more information about the DSD can be obtained by the dual-polarized variables. This case can be applied specially to the rainfall retrievals using a combination of the horizontal reflectively Z_h, differential reflectivity $Z_d r$ and the specific differential phase $K_d p$. Each of the three can provide a new information, at least, about the size of the hydrometeros.

$$ZDR = Z_h - Z_v \tag{6}$$

The ZDR can be expressed as the difference between the reflectivity in the horizontal eletromagnetic wave Z_h and the vertical Z_v. The ZDR depends on particle shape and falling behavior. Positives values of ZDR is caused by oblate particles falling oriented parallel to the polarization basis.

The correlation coefficient ρ_{hv} describes the correlation of the scatterring signal between horizontal and vertical polarization. A high correlation is expected if the orientation of particles does not change between pulses. For example, ρ_{hv} is almost 1 in rain, in strong rain 0.98 to 0.97. ρ_{hv} below 0.9 indicate irregular particules, and usually very below that non-meteorological targets.

The specific differential propagation phase KDP describes phase shift between the horizontal and vertical polarized wave. Phase measurements are not affected by attenuation nor needed to be calibrated, because it is based on the travel time of the propagation itself. But, precise KDP measurements required alternative integration over some distance (5 - 10 km).

3.2 Algorithm Theoretical Basis - DPSRI

Currently at Cemaden, the radar rainfall estimation is generated with the assumption that they represent the surface rain layer *(Dual Polarized Surface Rainfall Intensity - DPSRI)*. This methodology elaborates the rain fields considering the terrain topography within the radius range of the weather radar. Unlike some rainfall estimates that attribute reflectivities at an elevation angle (PPI) height (CAPPI), the SRI aggregates information from different elevation angles at varying heights. The Shuttle Radar Topographic Mission (SRTM) digital elevation model with 250 meters of horizontal resolution describes the topography that allows to classify the areas where the radar data can be considered invalid due to the interference of the electromagnetic pulse on the terrain. According to the algorithm, the rain is estimated from two fixed heights, in this case the Recife radar, between 500 meters and 5 km above the radar. The reflectivity data is interpolated between fields with different elevation angles (PPI) that form the DPSRI level (Figure 2). After establishing the reflectivity field at the DPSRI level, two Z-R ratios (Equation 7) are applied to estimate the radar radial domain precipitation. The adjustment of these reflectivity-rain ratios is based on [11, 2] classification of convective and stratiform rainfall. The algorithm is based on the volumetric reflectivity data applied to different indices of the Z-R ratio, depending on the scan height. So far, no correction is performed after estimating rainfall at the DPSRI level by the Z-R ratio.

$$Z = a.R^{b} \tag{7}$$

Where, Z is the reflectivity in (Dbz), R the rainfall rate (mm/h), a e b the coefficients.

To calculate the DPSRI it is applied a table according [10]. The DPSRI estimation consider the polimatric variables horizontal reflectivity (ZH), differential reflectivity (ZDR), specific differential phase (Kdp) and correlation coefficient (pdp) for some rainfall intensities. The a and b coefficients for the Z-R relation are the same as for SRI. The table was derived from [8].

$$R = \frac{R(Z)}{0.4 + 5.0|Z_{dr} - 1|^{1.3}} \quad for R(Z) < 6mm/h \tag{8}$$

$$R = \frac{R(Kdp)}{0.4 + 3.5|Z_{dr} - 1|^{1.5}} \quad for 6 < R(Z) < 50mm/h \tag{9}$$

$$R = R(Kdp) \qquad R(Z) > 50mm/h \tag{10}$$

where

$$R(Z) = \frac{1}{a^{1/b}} Z^{1/b} \tag{11}$$

$$R(Kdp) = 44.0|Kdp|^{0.822} \tag{12}$$

3.3 Radar Technical Information

The Table 1 is refereed to the technical characteristics of the Recife weather radar. The current spacial resolution is 0.5 km in each grid cell. The weather radar provides the reflectivity field at every 10 minutes. For this project it was also used the polarized variables: horizontal reflectivity (ZH), differential reflectivity (ZDR), specific differential phase (Kdp) and correlation coefficient (pdp).

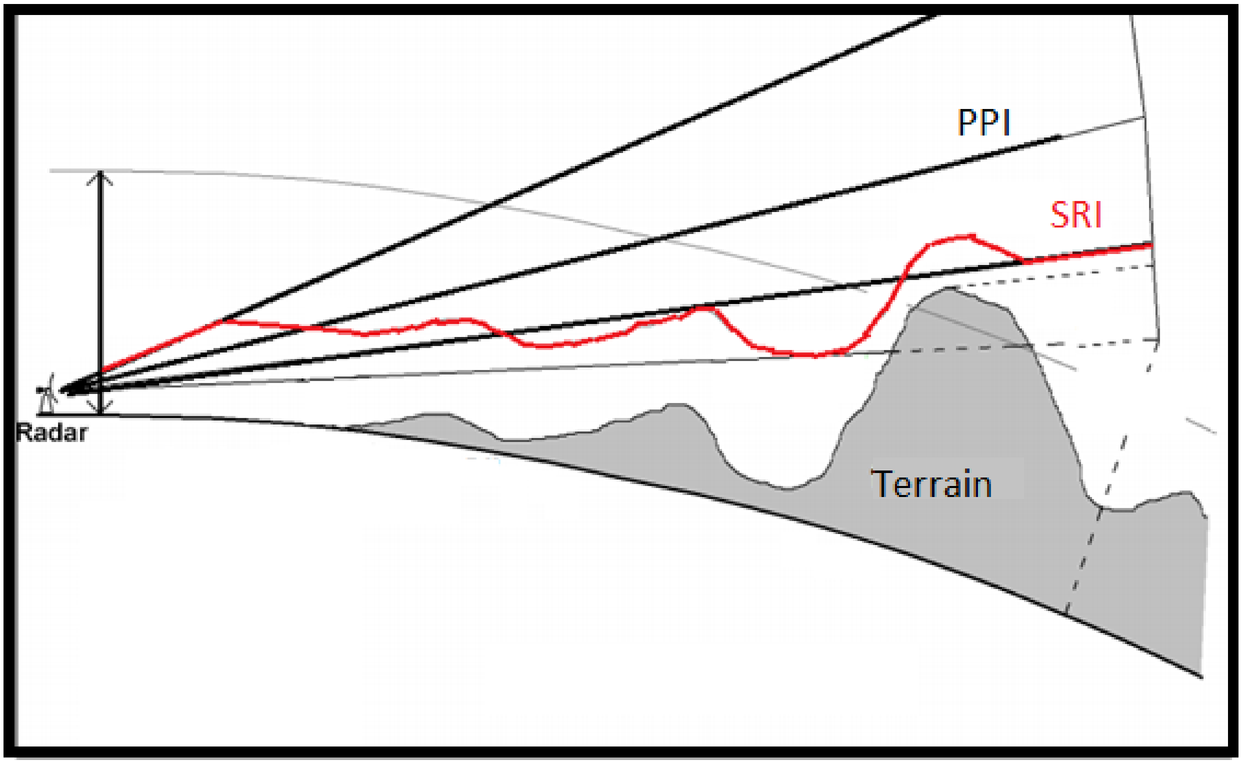

Figure 2: Representation of the DPSRI level (red line) from the elevation angles of the radar between two fixed heights. SOURCE: Adapted from [10]

Table 1: Technical characteristics of the Recife weather radar

Type	Dual-Polarized HV simultaneous
Band	S
Pulse Repetition Frequency (PRF)	600/480 Hz
Range bin.	0.25 km
Beam width	0.94
Quantitative Radius	250 km
Qualitative Radius	400 km
Number of Elevations	13 (from 0 to 20)
Company	SELEX

4 METHODS

It will be selected rainfall events during June and July of 2019. These months were chosen based on the rain season of the study region, and because there is no data before 2018, since the weather radar was recently installed.

The two rainfall data sets, from the rain gauges and weather radar, will be equally accumulated for 30 minutes, 1 hour and 1 day intervals. All the further analysis will be considered at these time intervals.

The main data generated using the weather radar (WR) and the rain gauges (RG) will be the matrix of error. The error will be calculated dividing the weather radar pixel value by the rain gauge value, at the same weather radar grid location, all divided by one. The result will be a multiplied factor which when applied to the original weather radar data will be able to reproduce an approximated value to the rain gauge. The key concept is how to interpolate the error, so the located error can be applied to all weather radar grid. It will be done using the error points as a conditional simulation to reproduce error field ensemble. An example of the methodology is shown at Figure 3.

In a geostatistical approach, the rainfall at a certain location in space is interpreted as a realization of a multivariate random variable. This random process is represented by a stochastic component that describes the spatial covariance structure of the deviations from this trend field. The random process is modeled based on a parametric semivariogram. In a semivariogram, the variance between rain gauges observations increases with increasing lag distance. After calculated, the semivariogram is applied in a geostatistical estimation method corresponding to the stochastic model, called conditional simulation. In this project the conditional simulation method will be used to interpolate the error and generate 30 realizations, all them considering the spatial structure derived from the semivariogram [12, 4, 3, 1]. It was divided part of the 237 total stations to validate the conditional simulations. The Figure 4 shows the 237 divided between 217 (blue dots) for simulations and 20 (red dots) for validation.

4.1 Analysis

First, It was calculate basic statistical indexes to evaluate the uncertainty of the weather radar to estimate the rainfall itself. The probability distribution function (PDF) for each time interval was also calculated to evaluate the temporal distribution of the rainfall intensities. A linear regression was applied between the rainfall estimated by the weather radar and the rain-gauges rainfall values, for each time interval.

The indices below are proposed to quantify the estimations uncertainties, or the budget error or the retrieval, by the Mean Absolute Error (MAE) (Eq. 13), Coefficient of Determination (R2) (Eq. 14).

$$\mathrm{MAE} = \frac{1}{N}\sum_{i=1}^{N}|S_i - O_i| \tag{13}$$

$$\mathrm{R2} = \frac{\sum_{t=1}^{n}(S_t - \bar{O})^2}{\sum_{t=1}^{n}(O_t - \bar{O})^2} \tag{14}$$

$$\mathrm{PBIAS} = 100\frac{\sum_{i=1}^{N}(S_i - O_i)}{\sum_{i=1}^{N} S_i} \tag{15}$$

$$\mathrm{NASH} = 1 - \frac{\sum_{t=1}^{n}(S_t - O_t)^2}{\sum_{t=1}^{n}(O_t - \bar{O})^2} \tag{16}$$

Where O_t are the observed values of rain gauges for validation and at a certain time t, $\bar{O}$ its mean e S_t the mean of the simulated values (DPSRI) for the same grid location. For accurate results, it is expected to obtain low values of MAE, PBIAS and high values of R2 and NASH.

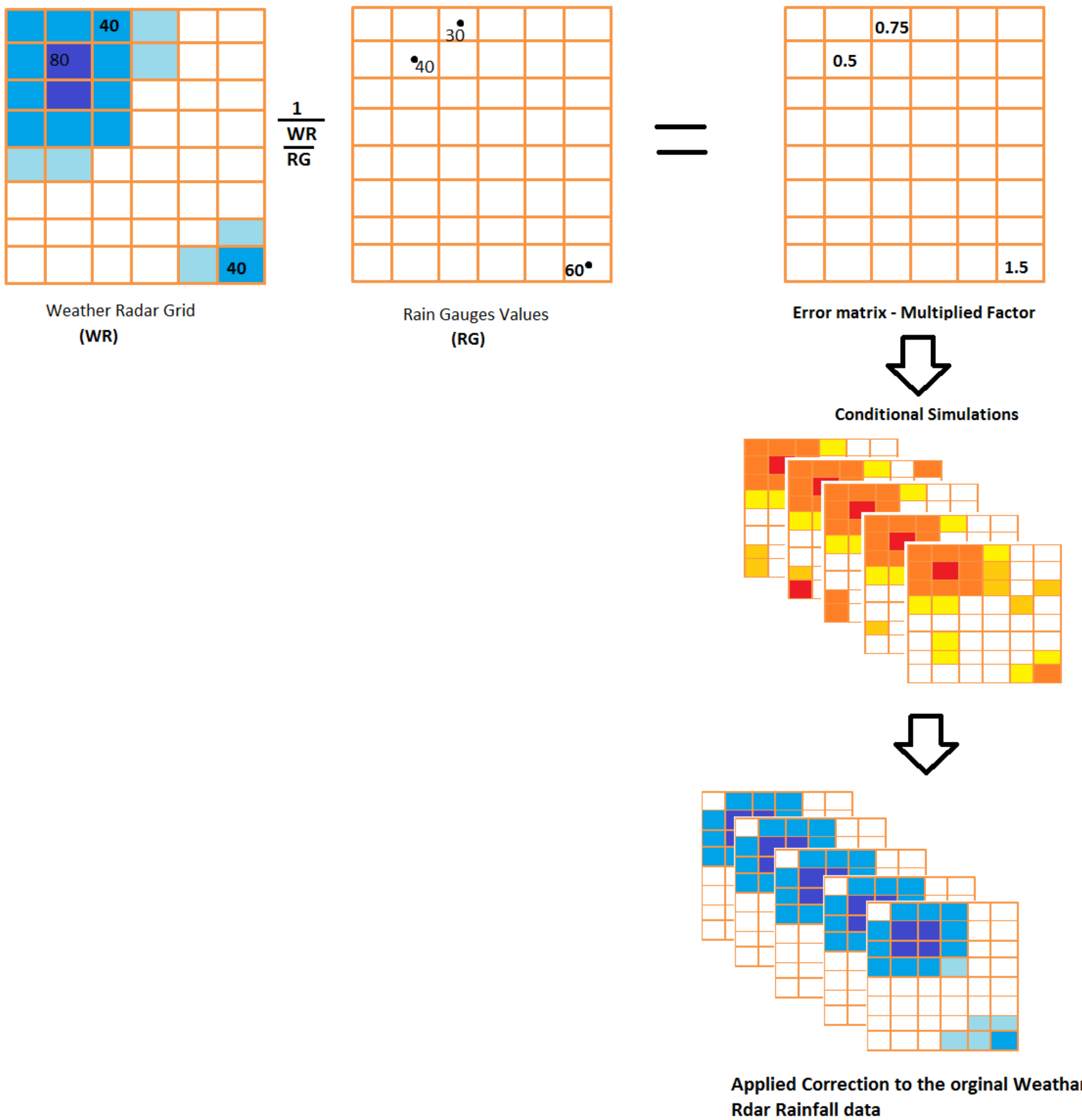

Figure 3: Methodology diagram

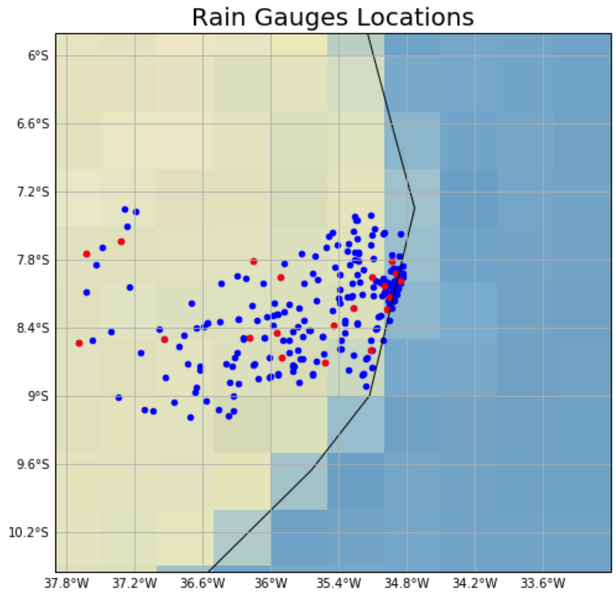

Figure 4: Rain gauges stations used to conditional simulations (217 in blue) and validation(20 in red).

5 RESULTS

5.1 Total Rainfall Accumulation

The Figure 5 shows the total accumulated rainfall from the weather radar and the rain gauges. The highest values of rainfall can be observed next to the coast. While the weather radar shows areas next to 56.3 mm/3days some rain gauges next to the same locations show values next to 200 mm/3days. From this map we clearly can conclude that the rainfall estimated by the DPSRI retrieval has been underestimated, compared to the rain gauge values.

5.2 Temporal Rainfall Series Distribution

In order to analyse the time series distribution over the 3 days period of analysis, the Figure 6 shows the accumulated rainfall comparing the mean value over all 237 stations for the rain gauges locations and the DPSRI (radar) values. It is also possible to notice that the rain gauge mean value of precipitation for every time step (30 minutes, 1 hour, 24 hours) is higher than the estimated by the weather radar. This graph is important to show that the distribution over time of the two variables are the same, the most intense values of rainfall at rain gauges and radar are the same. But the weather radar retrieval is underestimating the values at the rain gauges.

The Figure 7 shows the values of the Probability Distributed Function (PDF) with an exponential fit for the A) 30 minutes, B) 1 hour and C) 24 hours accumulated rainfall. The PDF shows that most current values of radar rainfall are close to zero rain, while the values at rain gauges are more distributed. The best exponential fit was for the rain gauge values.

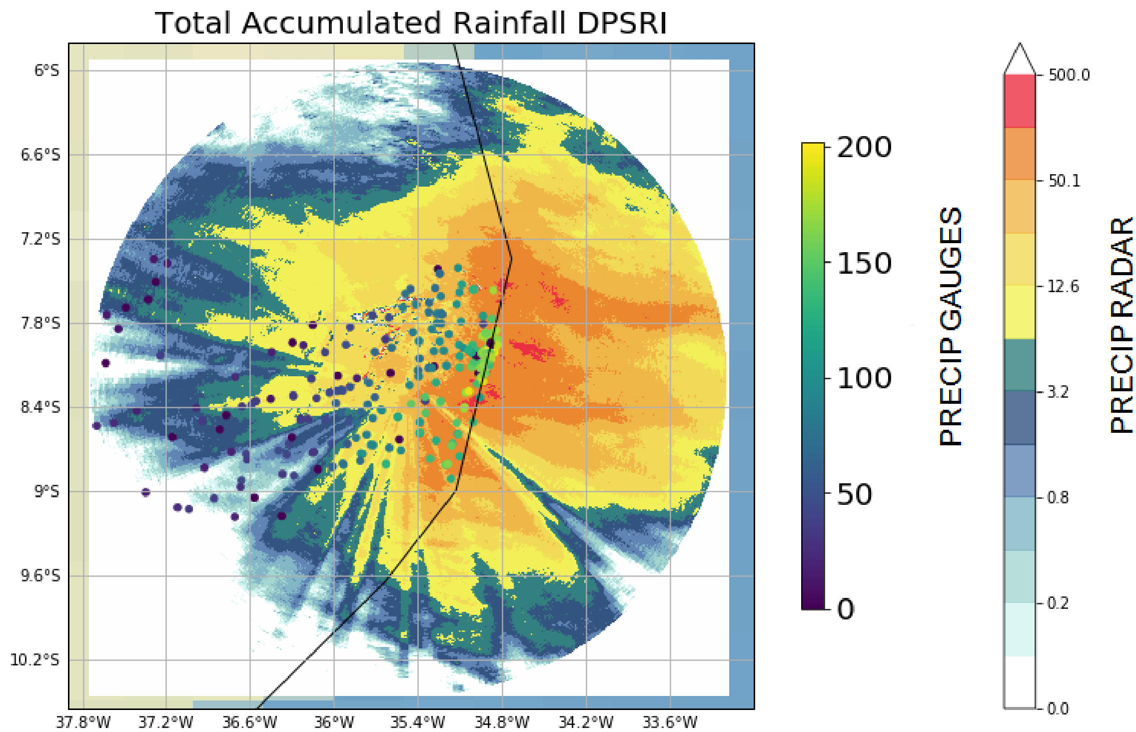

Figure 5: Total Accumulated Rainfall from 16 - 18 June 2019.

5.3 Linear Regression Analysis: DPSRI x Gauges

To analyse the linear fit between the rainfall retrieval and the rain gauge values, it was calculated the linear regression for each accumulated time step (Figure 8). The results shows a very poor fit between the variables.

5.4 Statistics metrics for DPSRI x Gauges

At the Table 2 is shown the statistical indices values between the rainfall estimated by the weather radar and the rain gauges. The values of median, 1Q and 3Q are also possible to be observed at the boxplots at Figure 9. The mean and the median values are very close to zero rainfall at 30 minutes and 1h accumulation, especially for the weather radar. The 24 hours accumulated values for the rain gauges are the one which presents the highest variance itself, the values are from 0 to 200 mm. Once more, the statistics shows that the weather radar have been understimating the rainfall. The NSE and R^2 values did not show a significant correlation between the two datasets, at any time-step.

Table 2: Statistics considering the 237 locations: Radar rainfall estimation and rain gauges.

	Mean	25 Q	Median	75 Q	Std	Var	R^2	MAE (mm)	MAE (mm/day)	PBIAS (%)	Nash-Sutcliffe (NSE)
gauge / 30min	0.61	0	0	0.6	1.35	1.82	0.06	0.5	24	-58.02	0.06
radar /30min	0.25	0	0	0.17	0.86	0.74					
gauge / 1h	1.21	0	0.2	1.57	2.31	5.34	0.09	0.96	23.04	-58.02	0.09
radar / 1h	0.51	0	0.03	0.44	1.44	2.07					
gauge / 24h	29.05	7.26	23.86	43.5	25.49	649.67	-0.38	20.19	20.19	-57.87	-0.38
rada / 24h	12.24	1.13	7.55	18.17	19.71	388.58					

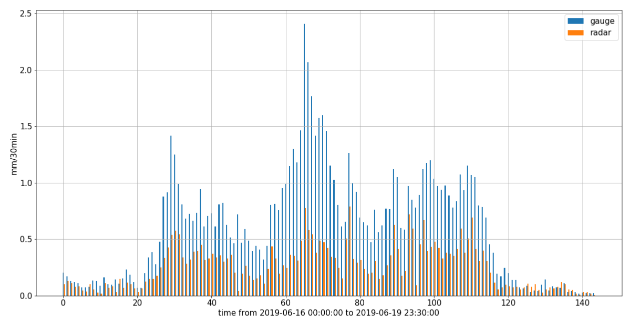

[A]

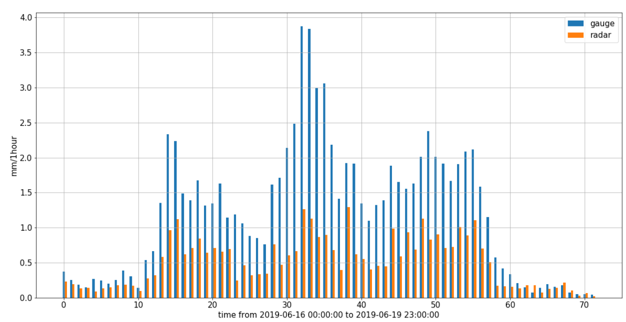

[B]

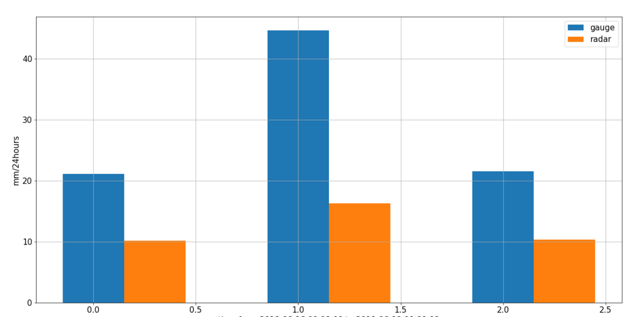

[B]

Figure 6: Time Series (mean over 237 rain gauges locations) for A) 30 minutes, B) 1 hour and C) 24 hours accumulated rainfall.

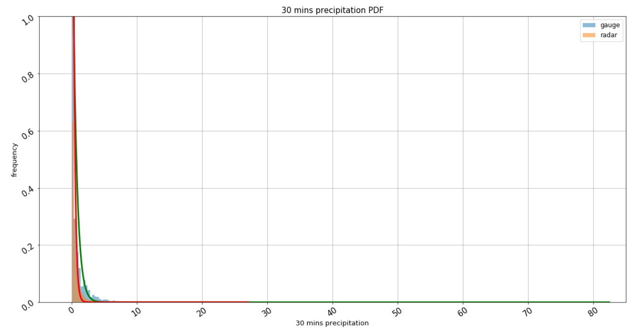

[A]

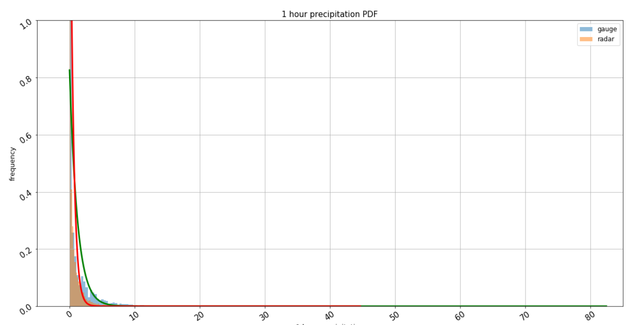

[B]

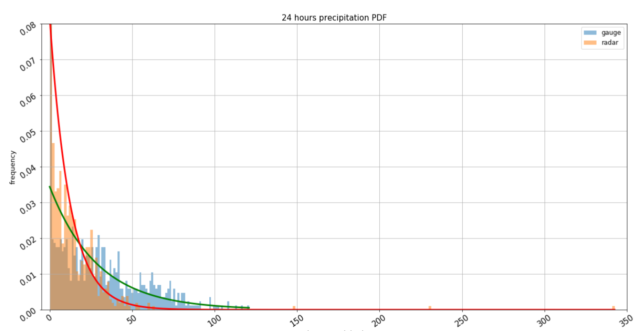

[B]

Figure 7: Probability Distributed Function (PDF) for A) 30 minutes, B) 1 hour and C) 24 hours accumulated rainfall.

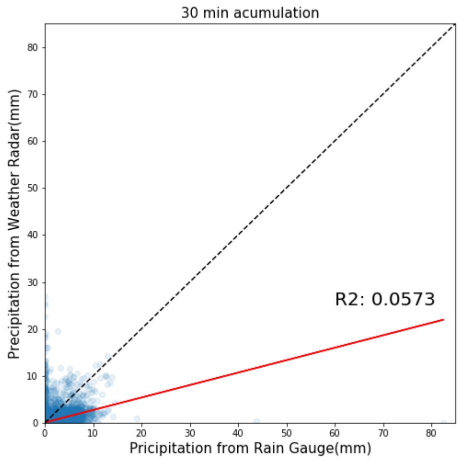

[A]

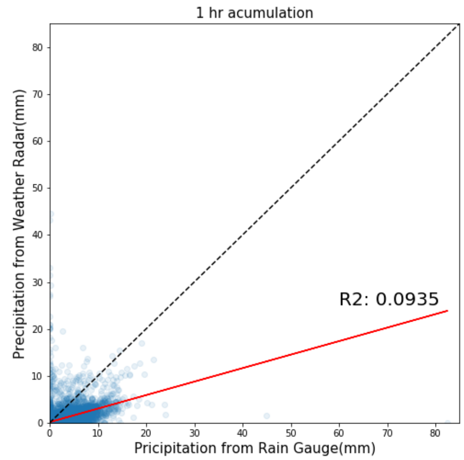

[B]

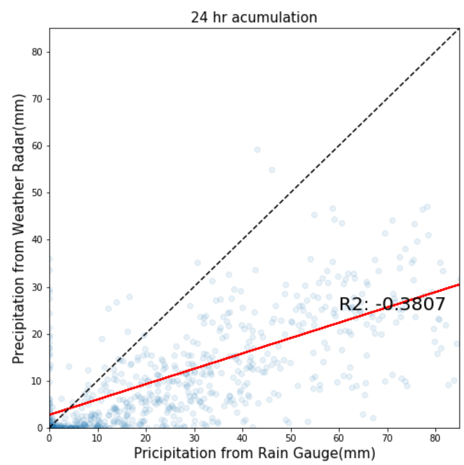

[C]

Figure 8: Linear Regression adjustment for A) 30 minutes, B) 1 hour and C) 24 hours accumulated rainfall.

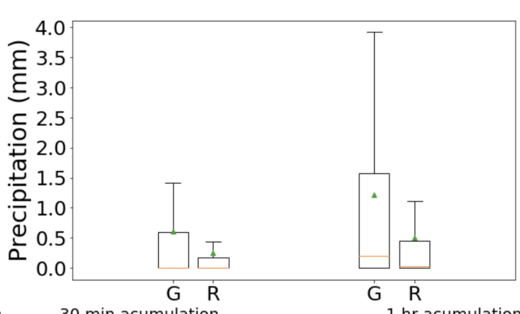

[A]

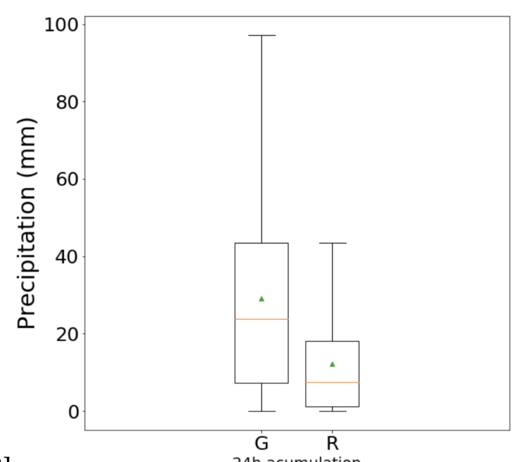

[B]

Figure 9: Boxplot for A) 30 minutes and 1 hour B) 24 hours accumulated rainfall

5.5 Ensemble with conditional simulations

By the time we had the middle results, we were only able to calculate the conditional simulations considering the 24 time steps, so 20 conditional simulations for each one of the three days. For each time-step it took 15 minutes to generate the 20 realizations. To generate 72 time-steps at 1h accumulation would take 18 hours. The Figures 10, 11 and 12 show the 20 realizations error maps for 16, 17 and 18 June 2019. The Figures 13, 14 and 15 show the respectively multiplication by the original rainfall data from the weather radar. It is possible to noticed that the multiplied factor helped to increase the values of precipitation.

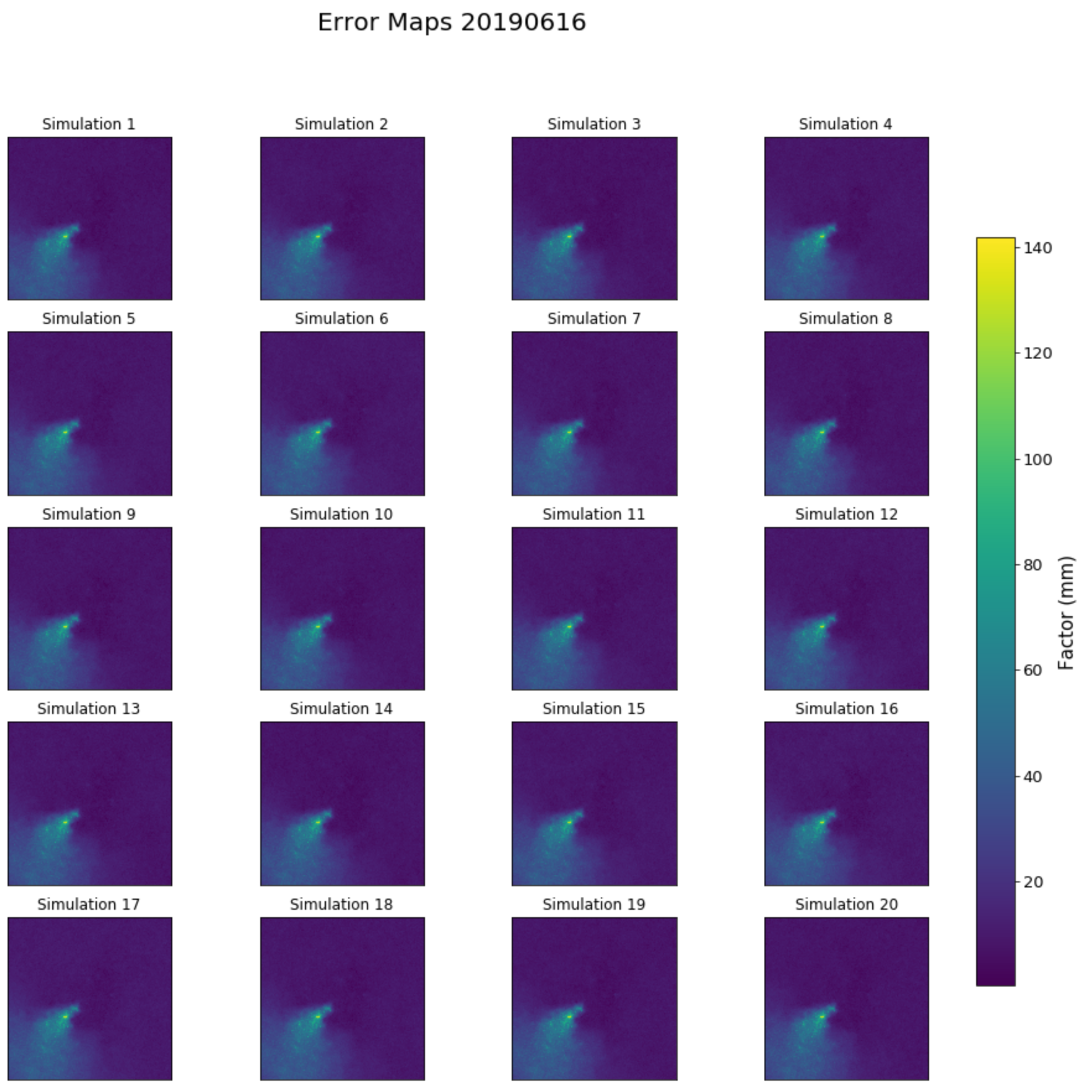

Figure 10: 20 realizations for error maps between the gauges and radar rainfall for 2019/06/16

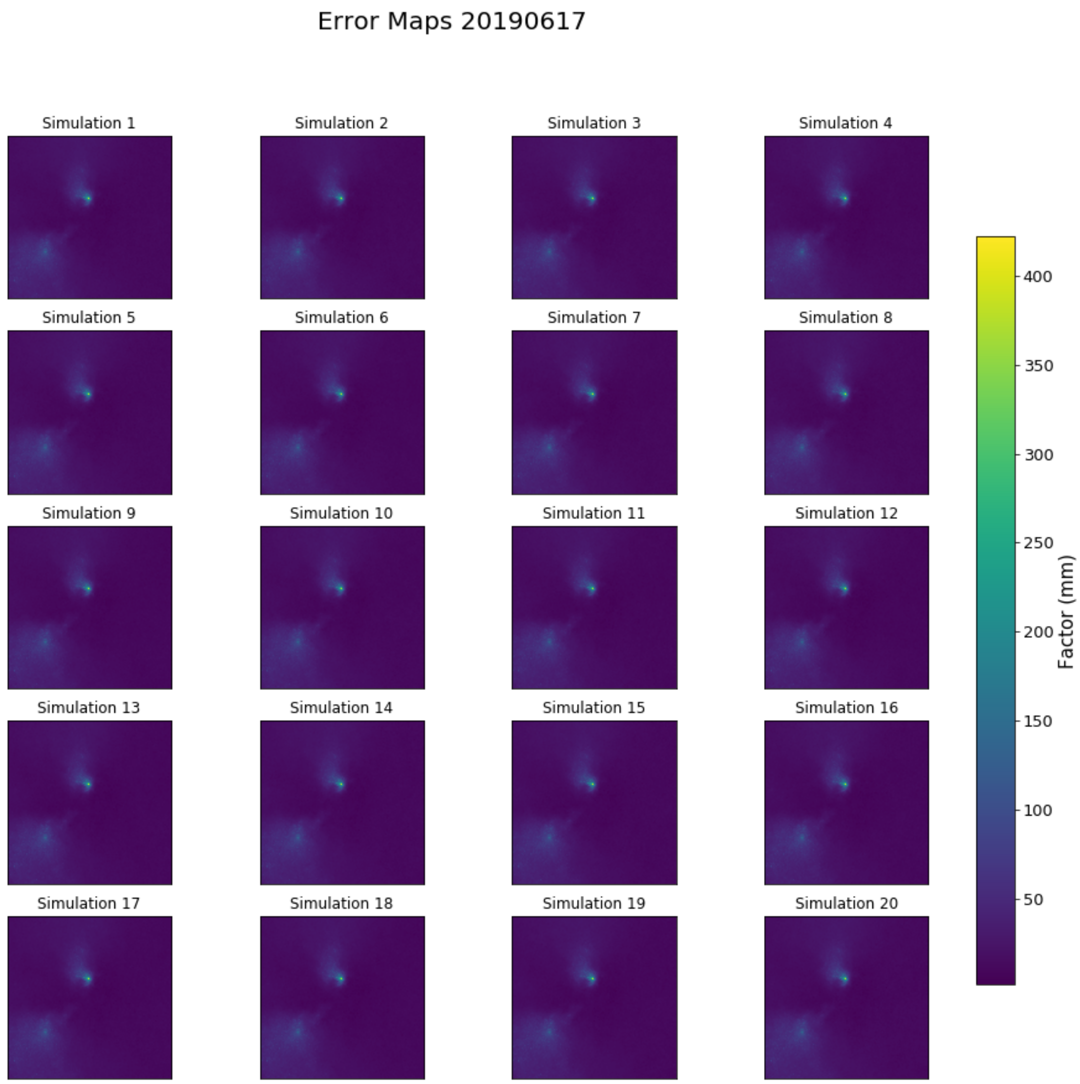

Figure 11: 20 realizations for error maps between the gauges and radar rainfall for 2019/06/17

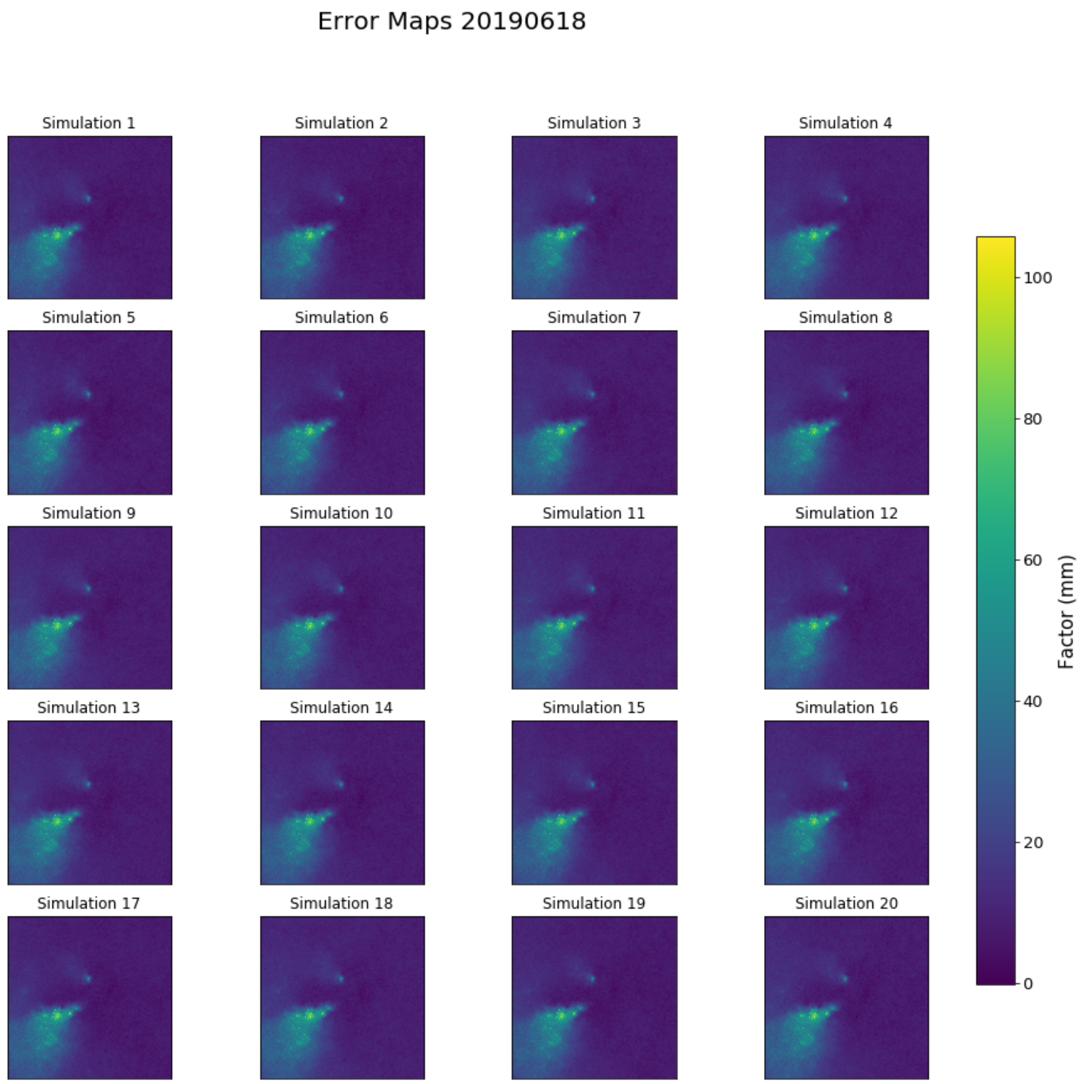

Figure 12: 20 realizations for error maps between the gauges and radar rainfall for 2019/06/18

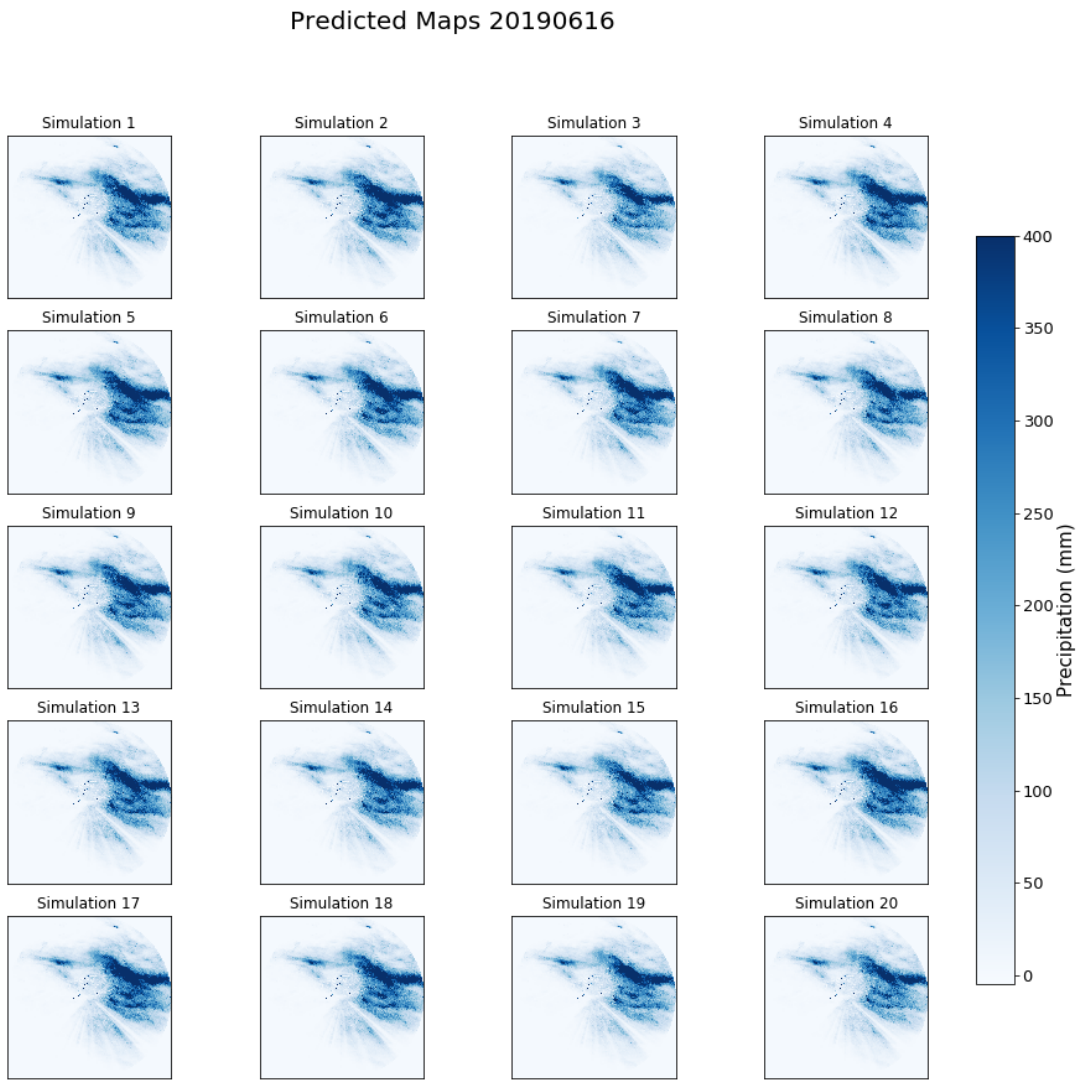

Figure 13: 20 realizations error multiplied by the original weather rainfall data for 2019/06/16

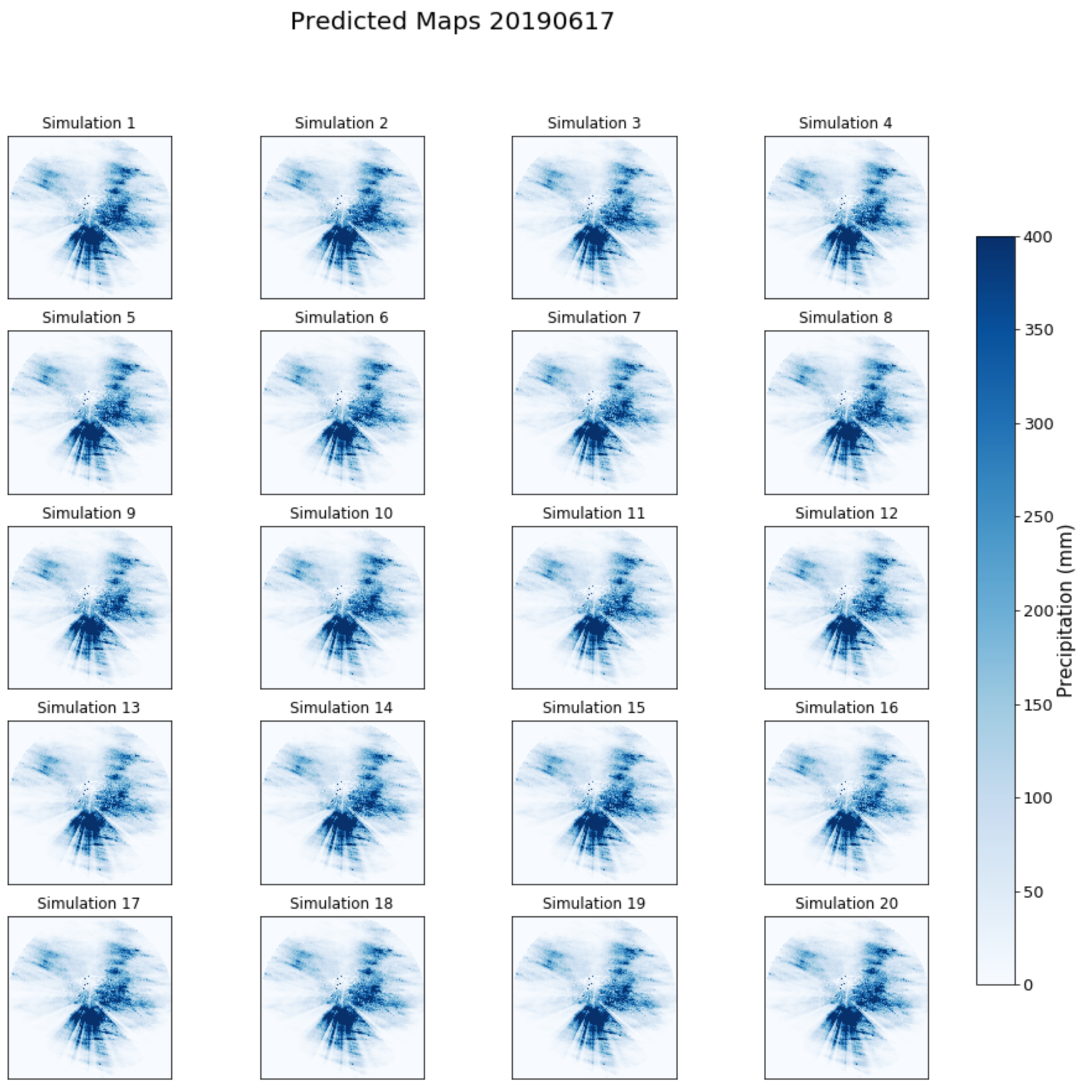

Figure 14: 20 realizations error multiplied by the original weather rainfall data for 2019/06/17

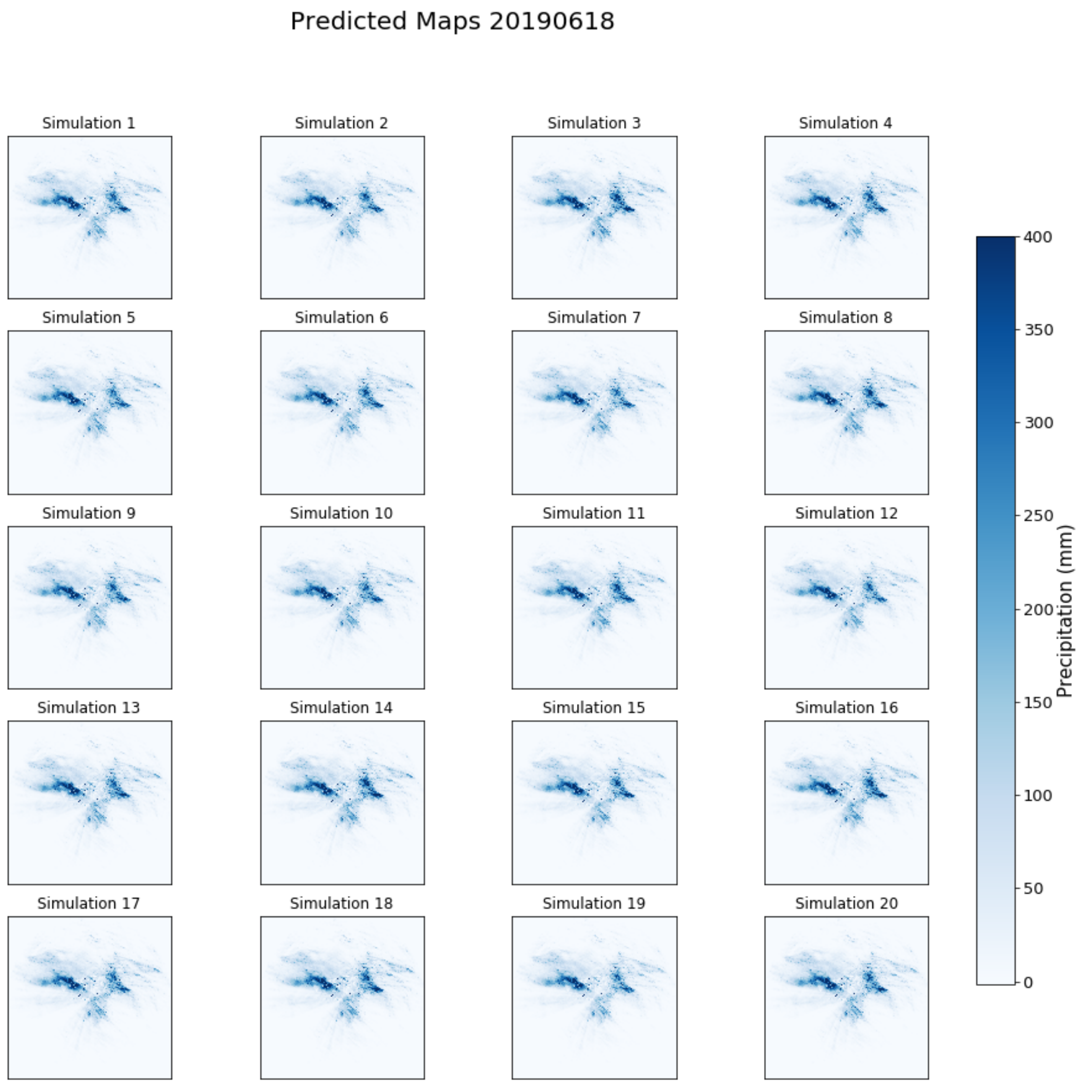

Figure 15: 20 realizations error multiplied by the original weather rainfall data for 2019/06/18

5.6 Semi-Variogram

A example of the semi-variogram used to calculated the 20 realizations are at Figure 16. It is different from what you had show at class, we think it is wrong because the axis seems inverted, but we moved on because we did not have time to fix it. The exponential fit is not even been showed.

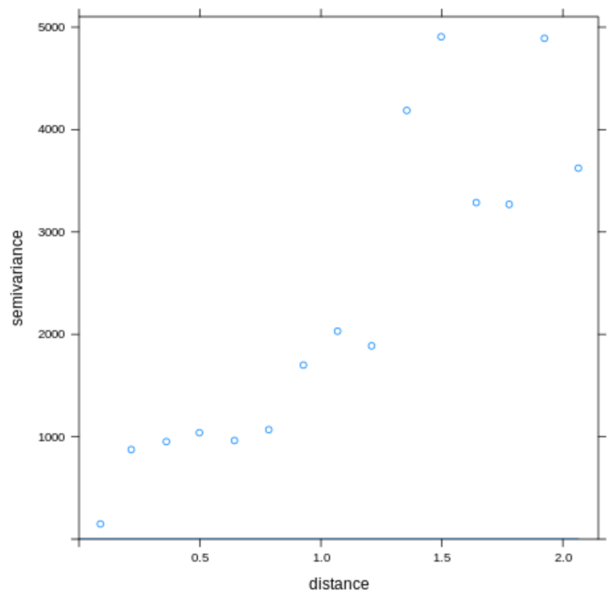

Figure 16: Semivariogram for 2019/06/16 - 24 accumulated rainfall error

5.7 Ensemble Mean Accumulation over time

To analyse if the multiplication factor was able to correct the rainfall underestimation of the weather radar, the Figure 17 show the accumulated rainfall of the ensembles for 3 rain gauges. The rain gauges locations were chosen based on the region the radar. The results shows that the mean of the ensemble (20 realizations) is overestimating the rainfall, at all stations shown. The best results was found for the station 12, where the spread of the ensemble could help the weather radar derived field to ge closer to the rain gauge rainfall value.

5.8 Linear Regression Analysis: Ensemble x Gauges

5.9 Statistics metrics for Ensemble x Gauges

At Table 3 is shown the statistics valeus considering only the 20 stations used for validating the method. The ensemble mean is the mean of the 20 rainfall realizations. It is possible to noticed that the ensemble mean is overestimating the rain gauges.

The Table 4 shows the error metrics (R^2, MAE, PBIAS and NSE) for among the ensemble mean, the original weather radar data and the rain gauge data. The results suggest the ensemble mean have been overestimating the rainfall, and the correlation between them is very poor. The Percentual Bias is positive and very high. But the PBIAS value is lower when compared with the rain gauge, which means that the method at least was able to approximate (too much) to the rain gauge rainfall values.

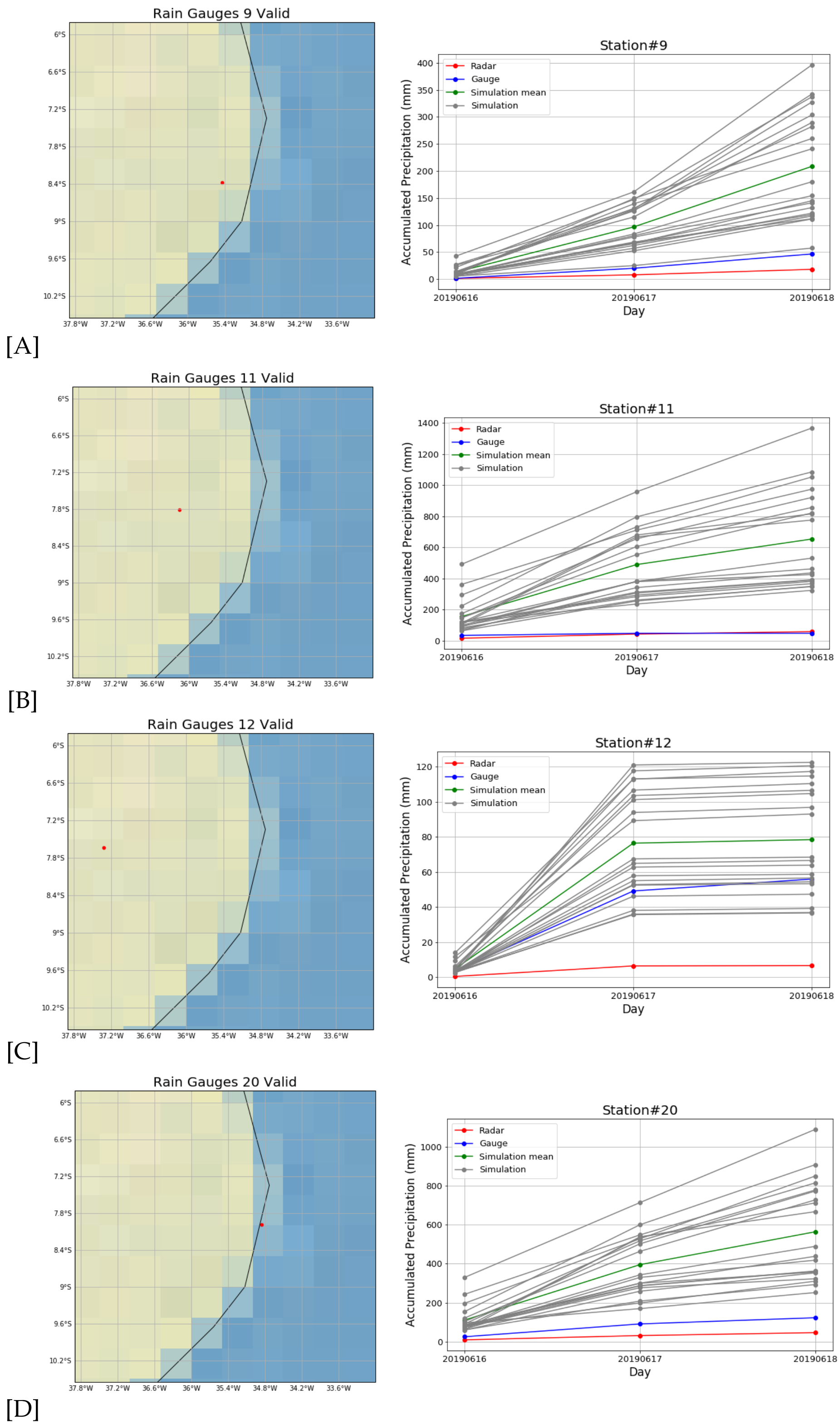

Figure 17: Accumulated rainfall series for for A) station 9 B) station 11 C) station 12 and D) station 20.

Table 3: Basic Statistics at the 20 rain gauge locations for validation of the method

	mean	1Q	median	3Q	std. dev.	variance
radar	13.16	1.09	10.02	22.42	13.79	190.27
gauge	29.05	6.09	25.2	49.5	24.97	623.65
mean ensemble	155.59	11.2	111.54	227.54	169.68	28791.38

Table 4: Error metrics for the ensemble mean rainfall

	R^2	MAE	PBIAS	NSE
radar and ensemble mean	-233.47	142.43	1082.17	-233.47
gauges and ensemble mean	-61.52	129.22	435.92	-61.52

6 CONCLUSION

The first result shows that the weather radar rainfall (DPSRI rainfall retrieval) have been underestimating the gauges rainfall, at every time-step of accumulated rainfall (30 minutes, 1h and 24h).

After the 20 realizations, the rainfall ensemble mean (for 24 h accumulated) was overestimating the rain gauge values, and also the original weather radar rainfall data.

We believe that the method worked to increase the radar rainfall value at the validation points, but there are some limitations. One of them could be the number of the stations available to apply the method. If the region were smaller or the number the stations were higher, we believe we could get better results.

7 PROPOSED WORK PLAN AND INDIVIDUAL ACTIVITIES

This is the list of the proposed work plan, the same written in the proposal document. It was difficult to separate the tasks because everybody worked at many of those topics at the same time. But some of us dedicated more to some topics. We believe that in the end the amount of work was equally separated to everybody.

- Transform the weather radar SRI binary data to netcdf (*Changpeng, Luiz, Sikai*)
- Accumulate the rainfall data into daily, hourly and 30 minutes intervals (*Luiz*)
- Read the rain gauges aascii text files and accumulate the data into daily, hourly and 30 minutes intervals (create a dictionary in python with the rain gauges). Be careful with missing data and possible instrument errors. (*Zilin, Luiz*)
- Transform the accumulated rain gauges data to netcdf (*was not necessary*)
- Extract the values of estimated rainfall (weather data) for rain gauges locations (*Luiz*)
- Make statistical analysis: histogram, boxplot, mean and standard deviation for each interval. (*Sikai, Changpeng, Zilin*)
- Apply a linear regression with the data and calculate the correlation between the two data sets for each interval. (*Sikai*)
- Analyze and explain the differences in rainfall intensity for each time interval and also the correlation between the data sets. (*Luiz, Sikai, Changpeng, Zilin*)

- Create a map of total accumulated rainfall from weather radar with the values of rain gauges over its locations. (*Luiz*)
- Explain the spatial variability of the rainfall over the Recife city, during the time period of the project. (*Luiz, Sikai, Changpeng, Zilin, it was shown by the animated gif*)
- Calculate error in each time step (weather radar over rain gauges values) (*Sikai, Changpeng, Zilin*)
- Calculate error semivariogram (*Zilin, Sikai, Changpeng*)
- Create 30 maps of error using a geoestatistical approach of conditional simulation method (*Zilin, Changpeng, in the end was only 20*)
- Apply the error map multiplying the values for in the original weather radar data (*Zilin, Changpeng*)
- Evaluate the rainfall rate for each time interval considering the rain gauges for validation (*Changpeng, Zilin*)
- Apply the same statistical methods as used before to compare the original weather radar and rain gauges, but this time considering the mean of the 30 ensemble simulations (*Changpeng*)
- Plots the accumulate graphs and see if the mean of the ensemble is closer to the rain gauges observations. (*Zilin*)
- Write on LATEX (*Luiz*)

REFERENCES

[1] B. Ahrens and S. Jaun. On evaluation of ensemble precipitation forecasts with observation based ensembles. *Adv. Geosci*, 2007.

[2] Michael I. Biggerstaff and Steven A. Listemaa. An improved scheme for convective/stratiform echo classification using radar reflectivity. *Journal of Applied Meteorology*, 39(12):2129–2150, 2000. doi: 10.1175/1520-0450(2001)040<2129:AISFCS>2.0.CO;2.

[3] A. T. DeGaetano and D. S. Wilks. Radar-guided interpolation of climatological precipitation data. *Int. J. Climatol.*, pages 29, 185–196,, 2008.

[4] R Erdin, C. Frei, and H. R. Künsch. Data transformation and uncertainty in geostatistical combination of radar and rain gauges. *J. Hydrol.*, pages 13, 1332–1346, 2012.

[5] U. Germann, M. Berenguer, D. Sempere-Torres, and M. Zappa. Real – ensemble radar precipitation estimation for hydrology in a mountainous region. *J. R. Meteorol. Soc.*, 2009.

[6] U. Haberlandt. Evaluation of radar-gauge merging methods for quantitative precipitation estimates. *J. Hydrol.*, pages 332, 144–157, 2007.

[7] O. Prat and A. Barros. Exploring the transient behavior of z-r relationships: implications for radar rainfall estimation. *Journal of Applied Meteorology and Climatology*, 2009.

[8] A. Ryzhkov, Giangrande S. E., and T. J. Schuur. Rainfall estimation with a polarimetric prototype of wsr-88d. *Journal of Applied Meteorology*, 44:502–515, 2005.

[9] J. M. Schuurmans, M. F. P. Bierkens, E. J. Pebesma, and R. Uijlenhoet. Automatic prediction of high-resolution daily rainfall fields for multiple extents: The potential of operational radar. *J. Hydrometeorol.*, pages 8, 1204–1224., 2007.

[10] SELEX. Rainbow 5 sofware manual - products and algorithms. *Selex ES GmBH Gematronik Weather Radar Systems*, Release 5.46.0:514, 2012.

[11] Matthias Steiner, Robert A. Houze Jr., and Sandra E. Yuter. Climatological characterization of three-dimensional storm structure from operational radar and rain gauge data. *Journal of Applied Meteorology*, 34(9):1978–2007, 1995. doi: 10.1175/1520-0450(1995)034<1978:CCOTDS>2.0.CO;2.

[12] Raphaela Vogel. Quantifying the uncertainty of spatial precipitation analyses with radar-gauge observation ensembles. *Scientific Report MeteoSwiss*,, pages 95, 80 pp, 2013.